Safety Evaluation of a Sodium-Ion Cell: Assessment of Vent Gas Emissions under Thermal Runaway

Arnaud Bordes, Guy Marlair, Aurélien Zantman, Alexandra Chesnaye,
Pierre-Alexandre Le Lore, Amandine Lecocq

Safety Evaluation of a Sodium-Ion Cell: Assessment of Vent Gas Emissions under Thermal Runaway

Arnaud Bordes, Guy Marlair*, Aurélien Zantman, Alexandra Chesnaye, Pierre-alexandre Le Lore and Amandine Lecocq
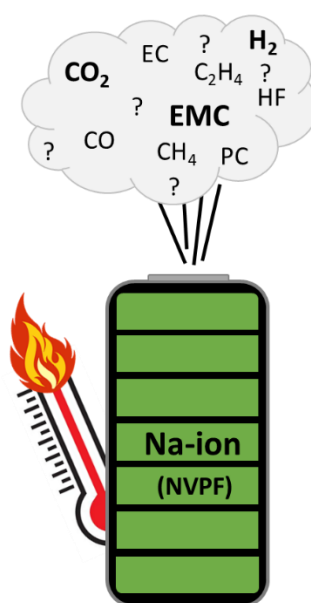
Institut National de l'Environnement Industriel et des Risques (Ineris), Parc Technologique Alata, BP2, 60550 Verneuil-en-Halatte, France

*corresponding author: guy.marlair@ineris.fr

Abstract

Na-ion batteries stand as a complementary technology to Li-ion batteries, that comply with the performance requirements of various applications without being submitted to the critical raw material dependencies pertaining to Li-ion. Several major industrial actors are now committed to produce these batteries, advocating among other, the safety gain of such technology. Available data on their behavior under thermal runaway are nonetheless very limited. This experimental work brings new elements on vent gas characteristics of Na-ion (NVPF) cells when thermally abused. A detailed gas analysis was performed in order to determine both composition of the gas mixture and related emitted volume. In our test configuration, no flames were observed, and the fumes were mainly composed of electrolyte compounds (organic carbonates). A simple comparison with Li-ion technology showed similarities with LFP chemistries in terms of nature and quantity of emitted gas.

TOC Graphic

For several years, Na-ion Batteries are being developed, these novel batteries being presented as a complementary technology to Li-ion batteries[1]. Even if their specific capacity is bound to be lower than that of Li-ion batteries, the key materials required for their manufacturing are different and often present in larger quantities and more evenly distributed on earth[2]. They are also reputed to be cheaper to produce and offer the possibility to use similar production lines as for Li-ion batteries[3]. Today the technology seems to approach maturity as several companies plan to market Na-ion cells in the coming months. This newcomer to the energy storage market will require adaptation of existing standards and regulations specifically created for Li-ion or other earlier technologies with different risk profiles. One example is the UN model regulation for the transport of dangerous goods which currently might request those cells to be transported under UN3292 entry, corresponding to Sodium battery whereas this entry was created considering the hydro-reactive behavior of Sodium batteries[4] (using metallic sodium). To avoid this problem, the creation of a dedicated UN entry for Na-ion cells batteries using organic electrolyte has just been decided[5] and several European countries just adopted a Multilateral Agreement (RID and ADR) dedicated to the transport of Na-ion batteries containing organic electrolyte[6]. Apart from this legal aspect, Na-ion producers often claim that the Na-ion technology is safer compared to Li-ion technologies[3]. Because the literature on this subject is scarce[7-14] and is often limited to thermal stability evaluation[12-14], this last point is rarely well sourced and still requires extensive and rigorous comparative study between different chemistries of each technology. Likely to Li-ion batteries, Na-ion batteries are subject to the well-known thermal runaway (TR) phenomenon. For Li-ion batteries, this phenomenon may produce severe hazards like fire, release of important amount of heat, projections and/or significant degassing[15-16].

Studies about Li-ion batteries degassing and related characteristics under TR conditions are ongoing for several years, pointing out complexity of this topic and difficulty to perform

detailed analysis[17] but also revealing potential toxicity and explosivity of the gas mix.[18-23] In this paper, we have used the experience achieved to develop Li-ion TR gas emission studies for producing early data concerning the characterization of Na-ion TR, targeting more particularly the assessment of the gas mix emitted in case of TR of Na-ion batteries.

To produce a fair amount of gas meeting the technical requirements for analysis purposes, TR event of six 18650 Na-ion cells were triggered simultaneously by overheating cells embedded in a dedicated copper support. The experimental set up is presented in figure 1. Four cartridge heaters were simultaneously used to ensure a homogeneous heating process. Temperatures and voltages of the cells were recorded to track thermal events and ensure that all the 6 cells entered into TR quasi-simultaneously.
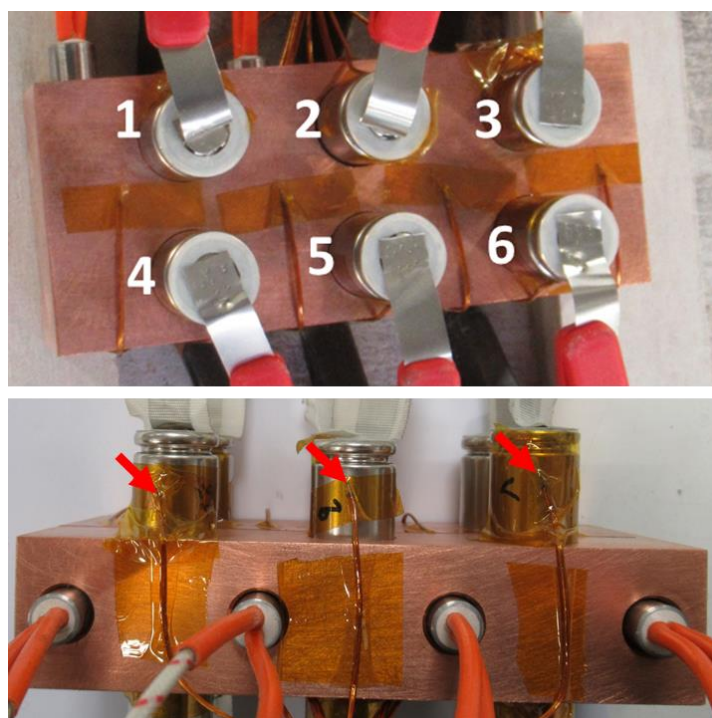

Figure 1: Experimental setup with the six cell assembly. Red arrows point at thermocouple location on cells 1, 2 and 3

As soon as the heaters were started (90 sec), the temperature recorded on the six cells increased. Cell temperatures plots are shown in figure 2. One hundred forty-seven (147)

seconds after the heaters were turned on, the temperatures recorded on the cells revealed fairly homogeneous (around 130°C). When the copper bloc temperature reached around 220°C (see details in supporting information (S2)), cell 1 entered into TR. Few seconds later, cells 3, 5, 6, 2 and 4 also entered in TR in this order. The time between thermal runaway of cell 1 and 4 was shorter than 15 s. The thermal runaway as reflected by temperature increase is concomitant with the voltage drop observed (S1) and the release of ethyl methyl carbonate (EMC) (figure 2), the most volatile solvent of the electrolyte, in the vent gas stream. A maximal temperature of 325°C (at 400 s) was recorded on cell 1, reflecting the absence of flaming combustion as confirmed by test video recording. Complete video recording is available in supporting information. Figure 3 presents time-framed image sequences selected from this recording.

Figure 2 : Evolution of temperature of Cells 1, 2, 3, 4, 5 and 6. Heaters are started at 100s and stopped at 400s.

Besides the confirmation of flameless degassing process, the video soundtrack allows to hear the opening of the cell vent (see video in supplementary information), just before a cell enters in TR. Figure 3 also reveals the apparition of large amounts of white fumes, concurrently appearing with temperature rise observed in figure 2. For the overall 6 cells, the degassing

5

process with white fumes lasted no longer than 40 s. Over the full duration of emission process, the gas mix was simultaneously pumped in order to be sampled and analyzed. The experimental set-up is presented in the experimental section. Pictures of four of the cells after the test are presented in supporting information (S4). Visual inspection shows limited degradation of the outside of the cells, except in the venting region. By contrast, the inside of the cells looks quite heavily degraded.

Figure 3: Extract from the video of the test before, during and after thermal runaway

Gas analysis

The result of the gas analysis is presented in table 1 and figure 4 in terms of mg/Wh and ml/Wh. The total emitted volume is 441 ml/Wh. For a single 18650 cell it represents 1,2 L. Both in terms of mass and volume, the organic carbonates contained in the electrolyte represent the most important species. EC/PC/EMC are found in coherent proportions with electrolyte composition. EMC is overrepresented in the gas mix due to its lower boiling point (107°C) compared with EC (248°C) and PC (242°C). Second most emitted compound is H_2 in terms of volume with a release of 45 ml/Wh, representing 10% of the total gas volume. Since no flaming combustion develops in our thermal abuse testing conditions, CO_2 and CO represent a small part of the gas mix (respectively 8 vol% and 1 vol%). Other gases formed and quantified include CH_4, C_2H_4 and HF. CH_4 and C_2H_4 might come from linear carbonates reduction and EC reduction respectively[15]. HF, for which emissions are often looked closely because of its known acute toxicity, represents 4 vol% (19 ml/Wh). Assuming most available source of fluorine in the cells originates from the electrolyte (meaning no significant conversion of F from PVDF binder nor from $Na_3V_2(PO_4)_2F_3$ cathode), a quick calculation based on its original quantity in the electrolyte shows that 1/3 of fluorine content is converted in HF: More in depth analysis would therefore be needed towards comprehensive understanding of the fate of fluorine in Na-ion under TR process. Despite the precautions taken to limit loss of signal, due to its high reactivity, some HF might have been lost in the sampling line and the filter leading to a possible underestimation.

Because POF_3 is sometime reported in the gas mix of Li-ion thermal runaway gas[21, 24-25], POF_3 was searched for but not found in the gas mix.

Species	mass (mg/Wh)	volume (ml/Wh)
EC	83	21
PC	250	55
EMC	1071	230
CO_2	71	36
CO	47	6
C_2H_4	33	26
HF	17	19
H_2	4	45
CH_4	2	3
Total	1577	441

Table 1 : quantified gas emissions. Other chemical species quantified but not detected are NO, NO_2, POF_3, CH_2O.

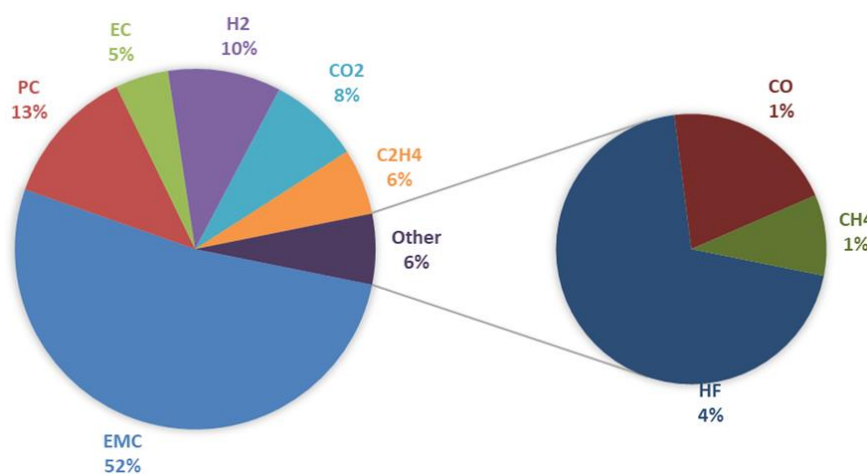**Figure 4 : chemical composition of the different quantified gases in mole fractions. Total volume is 441 ml/Wh in STP conditions**

In term of mass, the overall gas emission is 1.6 g/Wh, representing 4.1 g for one 18650 cell. The measured mass loss is 6.3 g per cell, which is in adequation with the total amount of electrolyte contained in one cell. The difference between the mass of emitted gas and measured

mass loss must come from emission of particles or electrolyte liquid drops, not accounted for by gas analysis.

Acknowledging that the analyzed gas mix contains an important part of flammable species (organic carbonates and dihydrogen), ignition of the gas mix would have greatly influenced the ultimate gas mix composition.

Comparison with Li-ion technology

In order to compare the gas emission analysis performed in this study on Na-ion cell with other results presented in the literature, a careful selection of published works had to be performed. Although several studies are available, only few are usable for relevant comparison, since not only methods and analysis protocols have to be consistent but also the cell reaction modes shall be comparable (leading or not to flaming combustion). Abuse tests where Li-ion cells react without flaming combustion are not common and, in this perspective, the best comparison basis identified is a recent study from our group[25] in which an NMC (111) pouch cell was abused by an internal heater and a study from Fernandes et al. where a LFP pouch cell was triggered into TR by overcharging the cell [19].

Both these studies used pouch cells which differ from 18650 cells on some aspects (thermal conductivity, heat exchange, presence of passive safety device…) but, in the view of this study focusing on gas emission, the reaction mode (degassing without combustion) was considered as the principal parameter for a fair comparison. The comparison of the molar percentages in the TR fumes reported by these studies is presented in table 2.

Comparing emissions from NVDF Na-ion (our study) with LFP Li-ion reported ones[18] reveals a gas mix composition in both cells very similar: 59 vol% of the gas mix from tested LFP cell is composed of organic carbonates (EMC/DMC), H_2 represents 9 vol% of the mix,

CO_2 and CO counts for 18 vol% and 2 vol % respectively. Fluorinated species (C_2H_5F, CH_3F, PF_3 and HF) account for 3.7 vol%.

On the contrary important differences exist when comparing our results relating to Na-ion against NMC cell. The carbonates species in the latter case are indeed present in much lower quantities, which is balanced by increased levels of CO and CO_2. This difference could be explained by the presence of oxygen in the NMC cathode that is more easily released than in the case of NVPF (or LFP) cathodes in which oxygen is stabilized in a phosphate group[26]. Gas mix emission from NMC TR is also marked by an important percentage of H_2. As based on HF emissions, fluorinated species seem to be emitted in a lower amount for NMC cell but this observation might be misleading since total volume of gas emitted in the case of NMC is much higher (see below) and, from a mass based quantitative viewpoint, they are of the same order of magnitude (5 ml/Wh for NMC vs 19 ml/Wh for Na-ion NVPF).

The maximal recorded temperature on the Na-ion cell body (averaged from the 6 cells) is 286°C, a value similar to the one measured on the NMC cell body (265°C) considered in this study. Temperature measured on the LFP cell tab (150°C) is lower. It has nonetheless to be noted that results on Li-ion cell presented in this study have been selected based on that they were reflecting non flaming combustion process conditions. This explains that relatively low maximal temperatures were recorded in that case (<300°C). In other conditions (leading to flaming combustion in connection with the thermal runaway event), temperatures close to 1000°C can be observed[27-28], influencing overall nature and quantity of gas emission (pyrolysis or combustion processes …). Sampling methodology also play a crucial role in the quantification of the different species and might explain some differences observed between studies.

Species	Molar %		
	Na-ion (NVPF)	Li-ion (LFP)	Li-ion (NMC)
Organic carbonates	70	59	20
H_2	10	9	17
CO_2	8	18	30
CO	1	2	25
CH_2	1	1	4
C_2H_4	6	4	1
Fluorinated species	4	4	0.4
Miscelaneous	0	3	3

Table 2: comparison of molar fractions of the different gas species contained in the TR driven gas mix of Na-ion (NVPF), Li-ion (LFP)[19] and Li-ion (NMC)[25].

Total gas volume measured for one 18650 Na-ion NVPF cell is 33 l/kg or 441 ml/Wh. When comparing the gas emission per mass of cell, Na-ion NVPF technology is once again closer to LFP (22 l/kg) than NMC (80 l/kg). But, because of its low specific energy, when comparing the gas emission per Wh, Na-ion NVPF became closer from NMC (540 l/Wh) than LFP (182 l/Wh). It has to be noted that many studies in other conditions[18, 27] report much higher volume emission of gas in the case of NMC/LMO blended cathode and NMC pouch cell.

In conclusion, in case of thermal runaway, the gas mix emitted by Na-ion NVPF cell under TR leading to non-flaming degassing process mostly contains compounds coming from electrolyte degradation. Globally the TR triggered degassing process in studied comparable conditions looks quite similar between Na-ion and LFP Li-ion cells, both in terms of nature and quantity or emitted gases (weight basis). This similarity between NVPF and LFP cell behaviors probably reflect similar stable bounding of oxygen contained in both cathodes in a phosphate group, limiting partial inner oxidation of other compounds which is known to potentially occur the case with NMC Li-ion chemistries. To fully assess safety of Na-ion technology, TR driven degassing phenomena should be further investigated, starting with the evaluation of other potential field failure scenarios (degassing associated with flaming combustion, effect of cell aging…) that might drastically modify the gas emission. The quest for safer Li-ion batteries for innovative applications has proven to be a never-ending story, as revealed by regular field incidents[29-31] and importance of the related research field. Likewise for Li-ion technology, safety of Na-ion technology challenges although perceived less severe, shall not be underscored. Na-ion technology is not limited to NVPF variant, innovation will likely promote advanced key materials (active materials of electrodes, electrolytes) in search of better functional performances. Moreover, and other parameters that are critical for safety assessment, like thermal and electrical stability of the cell should be further investigated[32].

Experimental methods

<u>Cell</u>

NVPF/hard carbon 18650 prototype cells of a capacity of around 700 mAh, nominal energy of 2.6 Wh corresponding to a specific energy of 74 Wh/kg were assembled by Tiamat (Amiens-France). The electrolyte consists of a mix between EC/PC/EMC and $NaPF_6$ salt. Like for Li-ion cells, the electrolyte weight represents around 20 % of total cell weight. The binder

used in the positive electrode is PVDF. Within the 72h before test, all cells were charged at 1 A (1.4C) up to 4.2 V corresponding to SOC100%.

<u>Abuse tests set up and measurements</u>

The heating device was built as the assembly of four cartridge heaters (400 W each) integrated on a plain copper block prepared with calibrated holes to maintain the 6 cells in close contact with the copper.

The choice to trigger 6 cells simultaneously was made in order to increase the amount of emitted gas and render the gas analysis more accurate.

Abuse test was performed in a 12 m^3 test chamber equipped with a ventilation system remotely piloted to fully extract gases in the exhaust system connected to a gas cleaning equipment (scrubber system). The test was performed under air with a flow rate in the test chamber of approximately 1 000 m^3/h.

Online gas sampling is carried out through a heated line (180°C) positioned on the extraction duct connected to various analyzers. A non-dispersive infra-red (NDIR) analyzer was used for CO_2 and CO, a paramagnetic measurement device for O_2, chemiluminescence apparatus for nitrogen oxides (NO_x), mass spectrometer for H_2, and a Fourier-transform infra-red (FTIR) spectrometer (Thermo Scientific Nicolet 6700, gas cell of 2 m) for further analysis of gases and vapors. The online FTIR apparatus provides quantitative information regarding gases released from battery thermal runaway such as organic carbonates (EC, DMC, EMC, etc.), hydrocarbons (CH_4, C_2H_4, etc.), aldehydes (OCH_2, CH_3CHO, etc.), carbon oxides (CO_2, CO), fluorinated species as HF and POF_3, and other species as HCN, NOx and SO_2 responding in the infra-red domain, according to adequate calibration processes. For pertinent exploitation of obtained FTIR spectra, characteristic wavenumber ranges for each component were selected

with the aim of limiting as far as possible interferences. The gas analysis methods followed the principles of ISO 19702 standard[33].

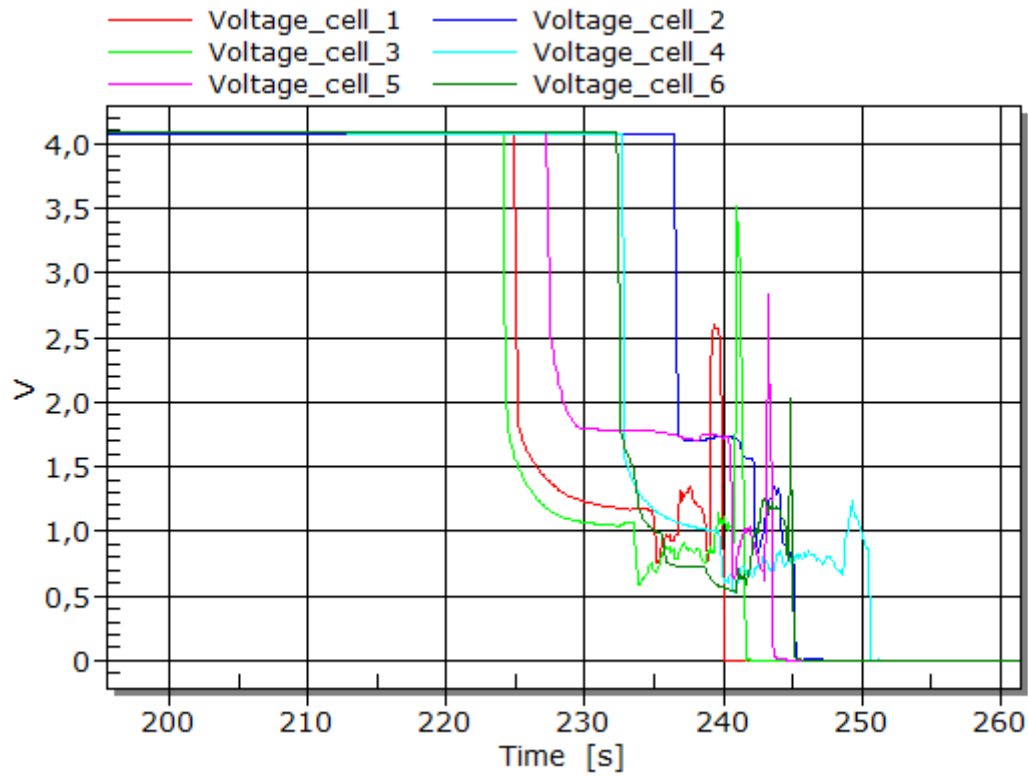**Supporting Information available**

- ➢ Video of the test
- ➢ Additional commented graphs (cell voltages, copper block temperature distribution)
- ➢ Picture of the cells after thermal runaway
- ➢ Table of some Na-ion developers/producers and related websites announcing commercialization plans

References

1.   Tarascon, J.-M., Na-ion versus Li-ion batteries: complementarity rather than competitiveness. *Joule* **2020,** *4* (8), 1616-1620.

2.   Yabuuchi, N.; Kubota, K.; Dahbi, M.; Komaba, S., Research development on sodium-ion batteries. *Chemical reviews* **2014,** *114* (23), 11636-11682.

3.   Bauer, A.; Song, J.; Vail, S.; Pan, W.; Barker, J.; Lu, Y., The scale-up and commercialization of nonaqueous Na-ion battery technologies. *Advanced Energy Materials* **2018,** *8* (17), 1702869.

4.   French-delegation, UN/SCETDG/55/INF.38 Sodium-ion batteries – comments on document ST/SG/AC.10/C.3/2019/35. *Committee of Experts on the Transport of Dangerous Goods, Fifty-fifth session* **2019**.

5.   https://unece.org/sites/default/files/2022-01/ST-SG-AC.10-C.3-118e.pdf, last access june 2022. *UNECE*.

6.   https://unece.org/transport/documents/2021/08/standards/multilateral-agreement-m340, last acceced june 2022. *UNECE*.

7.   Xia, X.; Dahn, J., Study of the reactivity of Na/hard carbon with different solvents and electrolytes. *Journal of the Electrochemical Society* **2012,** *159* (5), A515.

8.   Chayambuka, K.; Mulder, G.; Danilov, D. L.; Notten, P. H., From Li-Ion Batteries toward Na-Ion Chemistries: Challenges and Opportunities. *Advanced Energy Materials* **2020,** *10* (38), 2001310.

9.   Xia, X.; Obrovac, M.; Dahn, J., Comparison of the reactivity of Na_xC_6 and Li_xC_6 with non-aqueous solvents and electrolytes. *Electrochemical and Solid State Letters* **2011,** *14* (9), A130.

10.   Kuze, S.; Kageura, J.-i.; Matsumoto, S.; Nakayama, T.; Makidera, M.; Saka, M.; Yamaguchi, T.; Yamamoto, T.; Nakane, K., Development of a sodium ion secondary battery. *Sumitomo Kagaku* **2013,** *2013*, 1-13.

11.   Li, Y.; Hu, Y.-S.; Qi, X.; Rong, X.; Li, H.; Huang, X.; Chen, L., Advanced sodium-ion batteries using superior low cost pyrolyzed anthracite anode: towards practical applications. *Energy Storage Materials* **2016,** *5*, 191-197.

12.   Xie, Y.; Xu, G.-L.; Che, H.; Wang, H.; Yang, K.; Yang, X.; Guo, F.; Ren, Y.; Chen, Z.; Amine, K., Probing Thermal and Chemical Stability of Na x Ni1/3Fe1/3Mn1/3O2 Cathode Material toward Safe Sodium-Ion Batteries. *Chemistry of Materials* **2018,** *30* (15), 4909-4918.

13.   Zhao, J.; Zhao, L.; Chihara, K.; Okada, S.; Yamaki, J.-i.; Matsumoto, S.; Kuze, S.; Nakane, K., Electrochemical and thermal properties of hard carbon-type anodes for Na-ion batteries. *Journal of power sources* **2013,** *244*, 752-757.
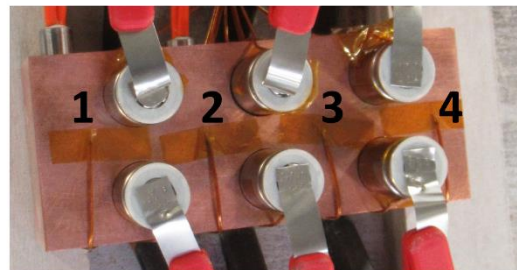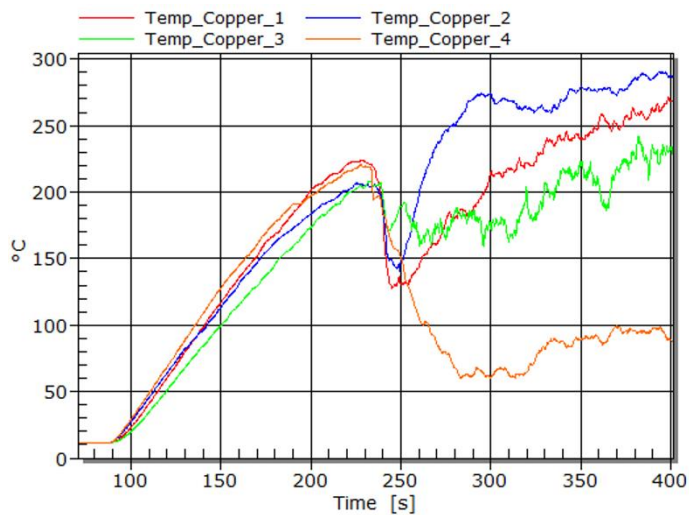
14.   Barpanda, P.; Liu, G.; Ling, C. D.; Tamaru, M.; Avdeev, M.; Chung, S.-C.; Yamada, Y.; Yamada, A., Na2FeP2O7: a safe cathode for rechargeable sodium-ion batteries. *Chemistry of Materials* **2013,** *25* (17), 3480-3487.

15.   Forestier, C.; Lecocq, A.; Zantman, A.; Grugeon, S.; Sannier, L.; Marlair, G.; Laruelle, S., Study of the Role of LiNi1/3Mn1/3Co1/3O2/Graphite Li-Ion Pouch Cells Confinement, Electrolyte Composition and Separator Coating on Thermal Runaway and Off-Gas Toxicity. *Journal of The Electrochemical Society* **2020,** *167* (9), 090513.

16.   Christensen, P. A.; Anderson, P. A.; Harper, G. D.; Lambert, S. M.; Mrozik, W.; Rajaeifar, M. A.; Wise, M. S.; Heidrich, O., Risk management over the life cycle of lithium-ion batteries in electric vehicles. *Renewable and Sustainable Energy Reviews* **2021,** *148*, 111240.

17.   Gachot, G.; Grugeon, S.; Jimenez-Gordon, I.; Eshetu, G. G.; Boyanov, S.; Lecocq, A.; Marlair, G.; Pilard, S.; Laruelle, S., Gas chromatography/Fourier transform infrared/mass spectrometry coupling: a tool for Li-ion battery safety field investigation. *Analytical Methods* **2014,** *6* (15), 6120-6124.

18.   Sturk, D.; Rosell, L.; Blomqvist, P.; Ahlberg Tidblad, A., Analysis of li-ion battery gases vented in an inert atmosphere thermal test chamber. *Batteries* **2019,** *5* (3), 61.

19.   Fernandes, Y.; Bry, A.; de Persis, S., Identification and quantification of gases emitted during abuse tests by overcharge of a commercial Li-ion battery. *Journal of Power Sources* **2018,** *389*, 106-119.

20.   Maloney, T., Lithium Battery Thermal Runaway Vent Gas Analysis Composition and Effect of Combustion. *Federal Aviation Administration* **2016**.

21.   Larsson, F.; Andersson, P.; Blomqvist, P.; Mellander, B.-E., Toxic fluoride gas emissions from lithium-ion battery fires. *Scientific reports* **2017,** *7* (1), 1-13.

22.   Kong, W.; Li, H.; Huang, X.; Chen, L., Gas evolution behaviors for several cathode materials in lithium-ion batteries. *Journal of power sources* **2005,** *142* (1-2), 285-291.

23.   Lecocq, A.; Bertana, M.; Truchot, B.; Marlair, G.; Verneuil-en-Halatte, F. In *Comparison of the fire consequences of an electric vehicle and an internal combustion engine vehicle*, Conference proceedings of Fires in vehicles, 2012; pp 183-193.

24.   Solchenbach, S.; Metzger, M.; Egawa, M.; Beyer, H.; Gasteiger, H. A., Quantification of PF5 and POF3 from side reactions of LiPF6 in Li-ion batteries. *Journal of The Electrochemical Society* **2018,** *165* (13), A3022.

25.   Bordes, A.; Marlair, G.; Zantman, A.; Herreyre, S.; Papin, A.; Desprez, P.; Lecocq, A., New insight on the risk profile pertaining to lithium-ion batteries under thermal runaway as affected by system modularity and subsequent oxidation regime. *Journal of Energy Storage* **2022,** *52*, 104790.

26.   Sapra, S. K.; Pati, J.; Dwivedi, P. K.; Basu, S.; Chang, J. K.; Dhaka, R. S., A comprehensive review on recent advances of polyanionic cathode materials in Na-ion batteries for cost effective energy storage applications. *Wiley Interdisciplinary Reviews: Energy and Environment* **2021**, e400.

27.   Yuan, L.; Dubaniewicz, T.; Zlochower, I.; Thomas, R.; Rayyan, N., Experimental study on thermal runaway and vented gases of lithium-ion cells. *Process Safety and Environmental Protection* **2020,** *144*, 186-192.

28.   Nguyen, T. T. D.; Abada, S.; Lecocq, A.; Bernard, J.; Petit, M.; Marlair, G.; Grugeon, S.; Laruelle, S., Understanding the thermal runaway of Ni-rich lithium-ion batteries. *World electric vehicle journal* **2019,** *10* (4), 79.

29.   Marlair, G.; Lecocq, A.; Bordes, A.; Christensen, P.; Truchot, B., Key Learnings From Recent Lithium-ion Battery Incidents that have impacted e-mobility and Energy Storage Fast Growing Markets. *Chemical Engineering Transactions* **2022,** *90*, 643-648.

30.   Zalosh, R.; Gandhi, P.; Barowy, A., Lithium-ion energy storage battery explosion incidents. *Journal of Loss Prevention in the Process Industries* **2021**, 104560.

31.   Sun, P.; Bisschop, R.; Niu, H.; Huang, X., A review of battery fires in electric vehicles. *Fire technology* **2020**, 1-50.

32.   Samigullin, R. R.; Drozhzhin, O. A.; Antipov, E. V., Comparative Study of the Thermal Stability of Electrode Materials for Li-Ion and Na-Ion Batteries. *ACS Applied Energy Materials* **2021,** *5* (1), 14-19.

33.   ISO 19702:2006 : Toxicity testing of fire effluents - Guidance for analysis of gases and vapours in fire effluents using FTIR gas analysis. **2006**.

S1 : Cell voltage variations as a function of time during the test

As can be observed, voltage drops are occurring with time differences not exceeding 12 seconds, showing adequacy and consistency of the testing protocol aiming at simultaneous TR activation of all cells.

S2 : Copper block temperature evolution versus time at 4 remote locations from the cells

Before activation of TR in the cells, temperature variation reflects homogeneous heating of the copper block due to high thermal conductivity of copper, since relatively narrow variation of all thermocouples 1 to 4 is observed. Once TR starts to be induced in the cell, and despite quasi simultaneous triggering of these events, more scatter is observed in the responses of copper block temperature distribution, due to fast thermal transfer of heat production within the cells in relation with sequential TR cascading processes. As a matter of fact, even small variations in TR activation in the cells are reflected through time shifted heat transfer processes in the block. The decrease of the temperature recorded few moments after TR might be due to partial loss of contact between copper block and thermocouples.
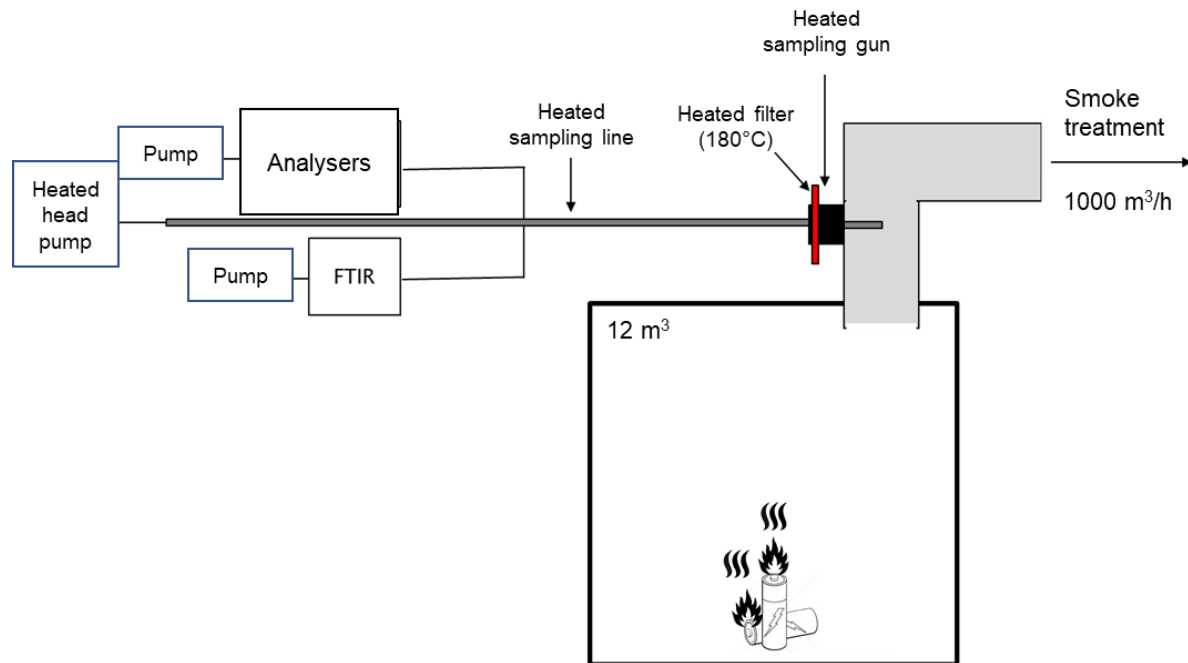
Company	Web link
CATL	https://www.catl.com/en/news/665.html
Natron	https://www.clarios.com/news-views/news-detail/2022/05/04/natron-collaborates-with-clarios-on-world-s-first-mass-manufacturing-of-sodium-ion-batteries#
Tiamat	https://www.eenewseurope.com/en/european-manufacturing-plan-for-sodium-battery-technology/
INDI ENERGY	https://indienergy.in/sodium-ion-batteries/

S3 : Short list of Na-ion promoters and related web links showing their commitment to short-term commercialization

S4 : Visual observation of thermal runaway induced degradation in four of the six tested cells.

Whilst external impact on the abused cells do not look very important, by contrast, inner content looks fully combusted.

S5 : experimental set-up for gas capture and sampling